Nanoparticles for bioimaging

Parvesh Sharma [a,b], Scott Brown [a], Glenn Walter [c], Swadeshmukul Santra [d], Brij Moudgil [a,*]

[a] Particle Engineering Research Center and Material Science and Engineering, University of Florida, Gainesville, 32611, USA
[b] Department of Chemistry, St. Stephen's College, Delhi University, India
[c] Department of Physiology and Functional Genomics, McKnight Brain Institute, University of Florida, Gainesville, FL 32611, USA
[d] Nanoscience Technology Center, Department of Chemistry and Burnett College of Biomedical Sciences, University of Central Florida, Orlando, FL 32826, USA

Abstract

The emergence of synthesis strategies for the fabrication of nanosized contrast agents is anticipated to lead to advancements in understanding biological processes at the molecular level in addition to progress in the development of diagnostic tools and innovative therapies. Imaging agents such as fluorescent dye-doped silica nanoparticles, quantum dots and gold nanoparticles have overcome many of the limitations of conventional contrast agents (organic dyes) such as poor photostability, low quantum yield, insufficient in vitro and in vivo stability, etc. Such particulates are now being developed for absorbance and emission in the near infrared region, which is expected to allow for real time and deep tissue imaging via optical routes. Other efforts to facilitate deep tissue imaging with pre-existing technologies have lead to the development of multimodal nanoparticles which are both optical and MRI active. The main focus of this article is to provide an overview of properties and design of contrast agents such as dye-doped silica nanoparticles, quantum dots and gold nanoparticles for non-invasive bioimaging.
© 2006 Published by Elsevier B.V.

Keywords: Non-invasive imaging; Fluorescence; Magnetic resonance imaging; Silica; Gold; Quantum dots; Multimodal; Nanoparticles

Contents

* Corresponding author. Tel.: +352 846 1194; fax: +352 846 1196.
  E-mail address: bmoudgil@erc.ufl.edu (B. Moudgil).

1. Introduction

A new era dawned in the history of medical diagnosis when Wilhelm Roentgen captured the first X-ray image of his wife's hand in 1896. Since the inception of X-ray technology for medical imaging, many non-invasive methodologies have been invented and successfully applied to fields ranging from clinical diagnosis to research in cellular biology and drug discovery. Biomedical imaging research has leveraged the benefits of significant advances in electronics, information technology and, more recently, nanotechnology. Substantial progress in the ability to fabricate particles in the "nano" regime (using both "top-down" and "bottom-up" approaches), and the discovery and understanding of their novel size dependent physical and chemical features [1] has drawn the attention of researchers in this area. The development of targeted contrast agents such as fluorescent probes has made it possible to selectively view specific biological events and processes in both living and nonviable systems with improved detection limits, imaging modalities and engineered biomarker functionality. These contrast agents have become a mainstay in modern medicinal and biological research with many reports now discussing the future scope [2,3] and commercialization [4,5] prospects. By the mid-2004, there were about 20,000 patents and patent applications in the field of nanotechnology with one of the areas of prime activity being nano-based biological and chemical detection [6]. The sales of medical imaging contrast agents reached $1.41 billion in 2003 and are expected to rise to $2.58 billion by 2009 in the US alone [7]. The fabrication of luminescent-engineered nanoparticles (with multifunctional features) is expected to be integral to the development of next generation therapeutic, diagnosis and imaging technologies.

2. Non-invasive imaging

A number of non-invasive optical imaging approaches such as computed tomography (CT), magnetic resonance (MR), positron emission tomography (PET), single photon emission CT (SPECT), ultrasound (US) and optical imaging (OI), including their variations and subcategories, have recently been described

[8–13]. Each differs in terms of sensitivity and resolution, complexity, time of data acquisition and financial cost. Different imaging techniques are, in general, complementary rather than competitive and the choice of imaging modality depend primarily on the specific question that is to be addressed. Imaging of biological specimens both in vitro and in vivo has long relied on light microscopy (fluorescence and luminescence imaging) and is currently attracting increasing attention as technological advances provide enhanced capabilities. Another technology that has grown remarkably as a tool in medical diagnostics, especially for soft tissues, is MRI. The development of multifunctional nanoparticles is a step further in the same direction. Multimodal nanoparticles [14,15] can be detected simultaneously by MRI and OI (e.g., fluorescence microscopy) as they incorporate the luminescent core and the paramagnetic ions (which generates MRI signals) into the same particle. Such particles integrate the advantages of high sensitivity (from optical method of detection, e.g., fluorescence) with the potential of true three dimensional imaging of biological nanostructures and processes at cellular resolution (i.e., MRI detection) [16–18]. Moreover, the limitations of each technique such as low sensitivity of MRI and limited anatomical background information acquired using OI are offset by one another. This chapter will briefly review the recent methods in imaging with a particular focus on optical imaging using luminescent nanoprobes, their design and applications in bioimaging.

2.1. Imaging modalities

Various modalities that have been used for non-invasive imaging in medicine are listed in Table 1.

A brief discussion of MRI and optical imaging contrast agents is presented below.

2.1.1. Magnetic resonance imaging (MRI)

The MRI technique is based on the basic principles of nuclear magnetic resonance. Essentially, it takes advantage of tissue contrast that is generated from the NMR signals received from hydrogen nuclei located in different physiological environments throughout an organism. When a specimen is placed within in a

Table 1
Non-invasive imaging modalities in clinical use

Imaging technique	Detection	Common contrast agents	Some clinical applications
Computed tomography	X-rays	Iopamidol, ioversol, iohexol, ioxaglate	Cerebral infarction, intracranial hemorrhage, angiography
Magnetic resonance imaging	Magnetic field	Gadoteridol, gadodiamide, gadopentetate dimeglumine	Cerebral and coronary angiography
Positron emission tomography	Gamma-rays	^{18}FDG, ^{15}H$_2$O, ^{68}Ga-EDTA, 11C-methionine	Cerebral blood flow and metabolic rates, degenerative diseases, brain development
Single photon emission computed tomography	Gamma-rays	^{99m}Tc-HMPAO, ^{99m}Tc-ECD, 111In-octreotide	Cerebral infarction, ischemia, dementia, cardiac imaging
Ultra-sonography	Ultrasonic waves	Microbubbles	Echocardiography, intracranial neoplasm, cephalic disorders

^{18}FDG: F-18 fluorodeoxyglucose.
^{68}Ga-EDTA: ^{68}Ga-labeled ethylenediaminetetraacetic acid.
^{99m}Tc-HMPAO: technetium-99m-D,L-hexamethylpropylene amine oxime.
^{99m}Tc-ECD: ^{99m}Tc-ethylcysteinate dimer.

Table 2
MRI parameters: factors influencing the signal from each location

Parameter	Description
T_1	Spin-lattice/longitudinal relaxation time. The T_1 relaxation time constant is a material property describing the characteristics of how this energy is given back to the surroundings
T_2	Transverse relaxation time. T_2 relaxation time constant describes the energy transfer between adjacent protons
T_2*	Same as T_2, but also contains heterogeneities in the environment
ρ	Spin density: the concentration of H nuclei in tissue

homogenous, static magnetic field nuclear spins will resonant at a given frequency that depends on the magnitude of applied magnetic field. Once the specimen has reached this equilibrium magnetization, it is then excited with a radiofrequency pulse at the appropriate resonant frequency resulting in a change in the net magnetization. When the radiofrequency pulse stops and the spins relax back to their equilibrium state, electromagnetic signals are transmitted back into the spectrometer. The changes in induced electromagnetic signals in the presence of linear field gradients are used to construct three dimension images of the body. MRI has excellent soft tissue specificity and can be used to identify many types of lesions in the brain and spinal cord. The predominant factors that influence the amount of signal and the extent of contrast received from a sample are listed in Table 2. The values of these parameters change from one tissue to the next and are responsible for the contrast between tissues of various types. Due to difficulties in distinguishing tumors from normal tissues in the body using an MR image, patients are often injected with contrast agents, such as gadolinium chelates and iron particles that selectively highlight the tumors. The design of MRI contrast agents is crucial since it helps to change the T_1 and/or T_2 of the protons in the vicinity of the agent and, thus, helps to generate image contrast (bright/dark) for diagnosis. According to the Solomon-Bloembergen-Morgan theory, which relates the observed paramagnetic relaxation rate enhancement to microscopic properties, proton relaxivities over 100 mM^{-1} s^{-1} for Gd^{III} complexes are predicted to be influenced the most by rotation, electron spin relaxation and water exchange on Gd^{III} [19].

2.1.2. Optical imaging

Light is the most versatile imaging radiation. It is non-invasive and able to create a contrast by intensity, wavelength, polarization [20], coherence, interference [21,22] lifetime and nonlinear effects. Optical imaging techniques (Table 3) have used different physical parameters of light interaction with tissues and the reader may refer to reviews written on the subject [23–29] for additional information.

Of the optical imaging techniques available, fluorescence microscopy has emerged as one of the most powerful imaging techniques. Optical fluorescence depends on the inherent property of the fluorophore (usually organic dyes, lanthanide compounds, etc.), which is illustrated in Fig. 1 (Jablonski diagram). When the fluorophore is excited by quanta of specific energy, it excites electrons from the ground state to a higher energy singlet state (S_1, S_2). Since different electrons have different energies (rotational and vibrational), the transition to a

singlet state demands change to an equivalent vibrational or rotational energy at a higher electrical state. During this process, the electron loses a part of its energy, generally through thermal decay (non-radiative energy decay) and, as a result, a lower energy photon is emitted. The difference between the wavelength required for excitation and the wavelength of the emitted light is known as the Stokes shift. This is the essential basis of all fluorescence methods. For instance, in fluorescence imaging, the energy from an external source of light is absorbed by the imaging agent injected near the tumor site (Fig. 2, step A) and almost immediately is re-emitted at a longer, lower-energy wavelength, which is detected by the detector (Fig. 2, step B).

The fundamental barriers to optical imaging of a tissue are high light scattering, autofluorescence and high absorption by hemoglobin (Hb) in the mid-visible band. Thus, depending upon the wavelength of light employed (typically restricted by the fluorophore used), different penetration depths can be achieved. For instance, UV–vis spectral range photons are strongly absorbed by the most relevant tissue chromophores, deoxy- and oxyhemoglobin (HbO$_2$), within the first few micrometers to a millimeter of tissue thickness, thus limiting its penetration. Near-infrared light of 650 to 900 nm, on the other hand, achieves the highest tissue penetration due to minimal absorbency of the surface tissue in this spectral region.

Table 3
In vivo optical imaging techniques

Technique	Contrast[a]	Depth	Commonly used wavelength	Clinical potential
Microscopic resolution				
Epi	A, Fl	20 μm	Visible	Experimental
Confocal	Fl	500 μm	Visible	Experimental
Two-photon	Fl	800 μm	Visible	Yes
Mesoscopic resolution				
Optical projection tomography	A, Fl	15 mm	Visible	No
Optical coherence tomography	S	2 mm	Visible, NIR	Yes
Laser speckle imaging	S	1 mm	Visible, NIR	Yes
Macroscopic resolution, intrinsic contrast				
Hyperspectral imaging	A, S, Fl	<5 mm	Visible	Yes
Endoscopy	A, S, Fl	<5 mm	Visible	Yes
Polarization imaging	A, S	<1.5 cm	Visible, NIR	Yes
Fluorescence reflectance imaging	A, Fl	<7 mm	NIR	Yes
Diffuse optical tomography	A, Fl	<20 cm	NIR	Yes
Macroscopic resolution, molecular contrast				
Fluorescence resonance imaging	A, Fl	<7 mm	NIR	Yes
Fluorescence molecular tomography	Fl	<20 cm	NIR	Yes
Bioluminescence imaging	E	<3 cm	500–600 nm	No

A: absorption, E: emission, S: scattering, Fl: fluorescence. Reprinted by permission from Macmillan Publishers Ltd: Nature Medicine (Ref. [23]), Copyright (2003).
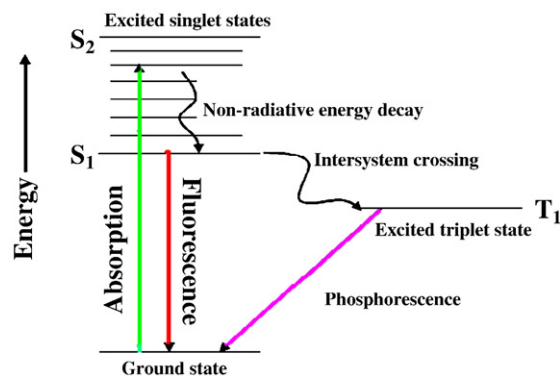
Fig. 1. A simplified Jablonski diagram.

This is because hemoglobin (the primary absorber of visible light) and water and lipids (the primary absorbers of infrared light) [30] have their lowest absorption coefficients in the NIR region [31] (Fig. 3). Deeper areas are thus accessible, permitting tomographic display of bulk tissue optical properties. Advanced fluorescence imaging techniques, such as fluorescence molecular tomography (FMT) [32–39] and fluorescence reflectance imaging (FRI) [40–43], commonly employ NIR wavelengths and, hence, are being scrutinized for in vivo molecular imaging applications. Weissleder group has recently shown that FRI and FMT using "smart" protease sensing probes not only permit detection of experimental spontaneous breast cancers but also differentiate breast cancers non-invasively [44]. Intravital microscopy (IVM) is another powerful tool for studying the molecular processes using fluorescent probes. In contrast to other optical imaging techniques, it allows continuous non-invasive monitoring of molecular and cellular processes in intact living tissues with 1–10 μm resolution [45–49].

2.2. Imaging agents

Imaging agents can be divided into following two broad categories.

Endogenous agents: These agents typically use an enzyme-mediated process inside the body to generate visible light when a substrate is degraded. The most commonly employed reporter systems are the fluorescent proteins, such as green fluorescent protein (GFP) (and its mutants) [50–54] and the luciferin/luciferase bioluminescent system [55–64]. GFP proteins require no further substances or substrates to work [26]. The excitation wavelength is 490 nm and there is only minimal photobleaching, which is a pre-requisite for the performance of long-term measurements [65]. This fluorescent pigment is covalently attached to the protein during synthesis. Consequently, the expression of the gene that encodes for GFP leads directly to the appearance of the green fluorescent signal, which is determined by the position of the mature protein [66]. Although fluorescent proteins offer an opportunity for extracting molecular and cellular level information in small animals, they have a less defined role in clinical applications [67–69]. A drawback of GFP is its low emission wavelength ($\lambda = 510$ nm), which overlaps with the autofluorescence of many tissues. Bioluminescence can be used to overcome some of the issues encountered with endogenous fluorophores. In bioluminescence imaging, a substrate (typically luciferin) is administered to an animal that has been designed to carry the luciferase (enzyme) such that when the substrate and enzyme meet, the luciferase is oxidized, emitting light, thus enabling detection. The application of bioluminescence for in vivo tracking is promising. However, current drawbacks include positional uncertainty of light emitting cells due to non-homogenous scattering, light penetration issues and an apparent need for a stable expression of luciferase.

Exogenous imaging agents: Exogenous agents are by far the most familiar contrast agents to today's researchers and scientists. They range from simple dyes used for colorimetric contrast to sensitive fluorescent probes and beyond. Examples of common exogenous agents and their respective imaging
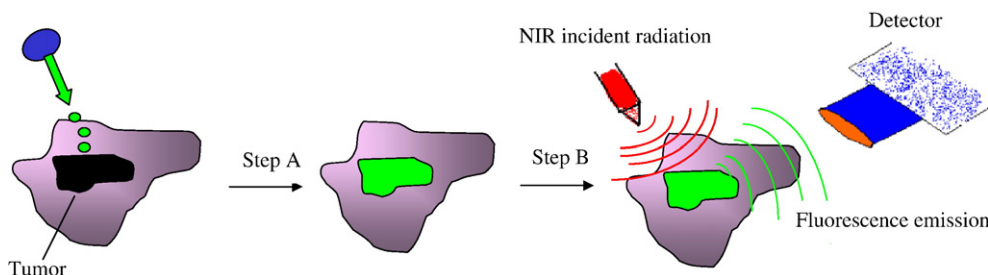

Fig. 2. Schematic representation of the application of the contrast agent on the tumor site (step A) followed by detection of reflected fluorescence emission from the contrast agent (step B).
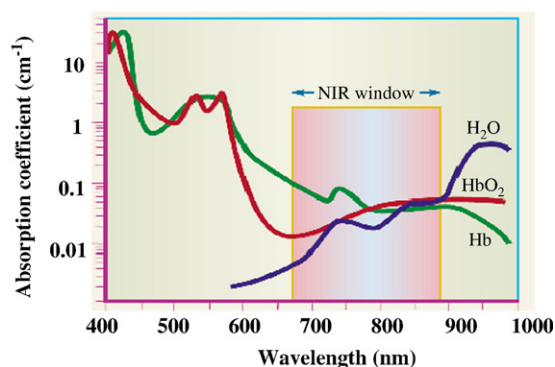
Fig. 3. NIR window (λ=650–900 nm) suitable for in vivo imaging. Reprinted by permission from Macmillan Publishers Ltd: Nature Biotechnology (Ref. [31]), Copyright (2001).

methods are lanthanide chelates and organic fluorophores used in fluorescence imaging, and gadolinium chelates and superparamagnetic iron oxide used in MRI. There are a number of limitations associated with the use of conventional contrast agents such as organic dyes and gadolinium chelates. In the next few sections of this review, we will identify key shortcomings and illustrate how innovations through nanotechnology have helped overcome these issues and open doors to new applications.

2.2.1. Issues with conventional contrast agents

Organic dyes: Organic fluorescent dyes are the most commonly used fluorophores. Dyes such as fluorescein isothiocyanate (FITC) and carboxyfluorescein diacetatesuccinimidyl ester (CFSE) have been used in various biological applications, such as fluorescent-labeled antibodies and molecules that are used to stain cells or organelles [70,71]. The main limitations of using organic dyes, however, are:

(i) They are prone to rapid photobleaching (i.e., they cannot fluoresce continuously for extended periods of time) and, thus, are unsuitable for extended periods of bioimaging observations [72,73].
(ii) Organic fluorophores are not well suited for simultaneous multicolor imaging applications. Most organic fluorophores have a relatively broad emission spectrum that can easily overlap with the emission of other fluorophores. Moreover, each fluorophore can be optimally excited only by a defined wavelength of light (which usually makes it necessary to use as many excitation sources as the types of fluorophores).
(iii) Emission/excitation is often susceptible to changes in local chemical environment (e.g., pH, interacting ions, etc.).
(iv) Emission from dyes can overlap with autofluorescence from tissues. The cause for autofluorescence in tissues is the presence of low amounts of fluorophores such as nicotinamide (NAD[H]), flavins, collagen and elastin [74]. The presence of these molecules gives background fluorescence that must be overcome when looking for signal derived from organic dyes, which unfortunately

often also fluoresce in the same region. This is a common shortcoming for the majority of dyes which fluorescence in the visible region. Because of this, exogenously administered fluorochromes that fluoresce in the NIR region [75–77], e.g., cyanine class of dyes, are now finding increased application in fluorescence imaging. However, most conventional dyes that emit fluorescence light beyond $\sim$850 nm suffer from low quantum yield (low brightness) and poor photostability [78,79].

MRI contrast agents: Many of the metals belonging to lanthanide and transition metal series have paramagnetic properties, which makes them likely candidates for MRI contrast agents. Materials with paramagnetic properties act indirectly to provide contrast enhancement by facilitating T_1 and T_2 relaxation processes via alteration of the local magnetic environment. Of the large variety of metals and compounds tested, Gd^{III} has been established as one of the best contrast agents due to its large magnetic moment. Currently, the most widely used MRI contrast agent is Gd-DTPA (diethyltriaminepentaacetic acid, DTPA is a chelating group which binds with the Gd^{III} ion); however, there are some issues concerning its applications:

(i) Although Gd-DTPA is now used widely as an MRI contrast agent, the uptake of Gd-DTPA in extravascular space (due to its rapid non-specific equilibration between the intravascular and extravascular space) as well as its unwanted enhancement of venous (and arterial) structures limits its potential.
(ii) Gd itself is toxic in ionic form with a half-life of several weeks. Although it is administered in a complex form, its stability is influenced by temperature, pH, concentration of surrounding ions and ligands. Moreover, endogenous metals, such as Zn and Cu, can displace Gd ion from the complex. Weinmann et al. have shown that some demetallation occurs in vivo with the deposition of free Gd^{III} ion in bones and liver, in cases of long residence time of Gd-DTPA in the body [80].

Besides, contrast enhanced MRI with gadolinium chelates suffers issues of timing [81], dose (e.g., better results were obtained with double dose of contrast medium to perform intraoperative MRI in patients with contrast enhancing intraparenchymal tumors of the central nervous system) [82], and surgically induced contrast enhancement [83] (i.e., enhancement that is caused by the surgical manipulation itself) which may be confused with residual tumor enhancement, thus leading to unnecessary further resection.

Among the transition metals commonly used, particle-based systems comprise superparamagnetic iron oxide (SPIO, 50–500 nm) or ultra-small paramagnetic iron oxide (USPIO, <50 nm). They have emerged as T_2 contrast agents, which permit negative contrast enhancement and, thus, darker images of the regions of interest. Magnetic nanoparticles of iron oxides [84,85] have been evaluated as an MRI contrast agent, especially for the liver and the spleen. However, relatively

high toxicity of magnetic nanoparticles restricts the use of these materials to human beings [86]. Iron particles and manganese complexes are not discussed in this review, but good summaries can be found in other sources [87,88].

2.2.2. Nanoparticle-based contrast agents

The important features of a fluorescence-based optical imaging agent are

a. In vitro and in vivo stability;
b. Resistance to photobleaching;
c. High quantum yield and high absorbency;
d. Resistance to metabolic disintegration and non-toxicity;
e. Emission in the NIR 700–900 nm window; and
f. Adequate dispersibility in the biological environment.

Additionally, for Gd-based MRI contrast agents, it is important that the Gd is permanently chelated to the largest extent possible. Free Gd^{III} is known to be toxic. In free (uncomplexed form), it binds to serum proteins and, consequently, most of it resides in the bone where it becomes tightly and irreversibly associated. The essential features involved in the design of the MRI contrast agents (Gd^{III} chelates) from the point of view of synthesis, kinetic and thermodynamic stabilities, higher relaxivities, water exchange, etc. have been described in detail [89,90]. To limit the toxicity due to non-specific uptake of the contrast agent, it is desirable that the imaging agent be sequestered preferentially at the targeted site.

Nanoparticle-based optical contrast agents such as quantum dots (QDs), gold nanoparticles, organically modified dye-doped silica, up-converting phosphors and lanthanide-based contrast agents are recent additions to the list of exogenous contrast agents which combine a number of desired features listed above. Out of these, the advantages of organically modified dye-doped silica nanoparticles (including those having multimodal functionalities), QDs and gold nanoparticles are discussed below.

2.2.2.1. Dye-doped silica nanoparticles.

As discussed above, rapid photobleaching is one of the problems with organic fluorescent dyes. Numerous photochemical reactions occur in the cellular environment that can lead to photodegradation of the dye [91,92]. The encapsulation of the dye in a ceramic matrix is one methodology presently in use to maximize both in vitro and in vivo stability. This minimizes oxygen access, increases chemical stability and allows surface modification of the shell to enhance hydrophilic character and cell uptake. Different techniques that are in use for encapsulation include incorporation in nucleic acid and PNA oligomers [26], lipid micelles [30,76,77,93,94], polymer matrices and encapsulation in silica matrix [15,95–102].

2.2.2.1.1. Basis of optical detection.

For these composite systems, the 'dye' encapsulated within the matrix of the nanoparticles is the source of the fluorescence. The encapsulation process may alter the fluorescence emission of the dye (e. g., the emission maximum) marginally but offers many advantages. Capturing of dye within the core prevents the dye

from rapid photobleaching [96,103] as it is prevented or delayed from coming into direct contact with the chemicals in the surrounding environment. Santra et al. [103] have recently described a novel fluorescence lifetime-based approach to determine the core-shell structure of the dye (fluorescein isothiocyanate)-doped silica nanoparticle. It is revealed that approximately 62% of dye molecules remained in the solvated silica shell, while 38% of dye molecules remained in the non-solvated (dry) silica core. This allows imaging process to be performed over extended periods of time.

2.2.2.1.2. Properties.

The interest in the use of silica-coated particles as biomarkers is increasing because of multiple reasons:

(i) Amorphous silica appears to be a biocompatible [104] and non-toxic [105] material.
(ii) The outer silica shell allows tuning of the interaction potential between the particles (thus influencing their aggregation behavior).
(iii) Silica matrix is optically transparent [106] that allows excitation and emission light to pass through the silica matrix efficiently.
(iv) Fluorescent dyes can be effectively entrapped inside the silica particles [107] and the spectral characteristics of the dye molecules remains almost intact. Silica encapsulation provides a protective layer around dye molecules, reducing oxygen molecule penetration (that causes photodegradation of dye molecules) both in air and in aqueous medium (in this case dissolved oxygen) [96,103]. As a result, photo-stability of dye molecules increases substantially in comparison to bare dyes in solution.
(v) Facile routes are available to encapsulate the dye, e.g., the dye can be encapsulated in a reverse micellar medium or the dye can also be attached to the silica using a modified Stober's process.
(vi) The size of silica particles remains relatively unchanged by changing solvent polarity (i.e., resistant to swelling) and, therefore, silica porosity remains unaltered in a wide variety of solvents.
(vii) The surface of silica particles can be easily modified to attach biomolecules [96,97,108] such as proteins, peptides, antibodies, oligonucleotides, etc., using conventional silane-based chemistry. For example, carboxylated silica nanoparticles can be covalently attached to the amine groups of proteins, antibodies, etc., via the formation of a stable amide bond [109] and peptides containing cysteine residue (via-S-H group) can be attached to the aminated silica nanoparticles [110].

2.2.2.2. Quantum dots.

Quantum dots (QDs) are semiconductor crystals with all three dimensions in the 1–10 nm size range that luminesce due to quantum confinement effects. QDs provide a new class of biomarkers that could overcome the limitations of organic dyes. The use of QDs as luminescence probes in cell imaging has increased significantly since the first examples from Alivisatos [73] and Nie's groups [111]. In many respects, these luminescent nanocrystals behave like a transitional stage between bulk semiconductors and single atoms. In

this size regime, the electrons exhibit quantum mechanical effects [112–119].

2.2.2.2.1. Basis of optical detection. The most useful outcome of quantum confinement–for the applications discussed in this paper–is the discretization of the energy levels at the edges of both conduction and valence bands upon dimensional (size) reduction. This can briefly be explained as follows. In extended semiconductors, the overlap of atomic orbitals leads to the formation of valence and conduction bands separated by an energy gap. Upon excitation of a semiconductor, an electron is promoted from the filled valence band to the largely empty conduction band. This creates a positive vacancy "hole" in the valence band. The spatial separation (Bohr radius) of this electron-hole pair ("exciton") is typically of the order of 1–10 nm for most semiconductors and quantum confinement arises when one of the dimensions of the object becomes of the order of the exciton Bohr radius. Thus, in QDs, the excitons are confined in a way similar to a particle-in-the-box problem leading to a finite band gap and discretization of energy levels. This separation (band gap) depends upon the number of "atoms" joining together to form the band and, thus, is a function of nanocrystallite size. Fluorescence of semiconductor nanocrystals is due to the radiative recombination of an excited electron-hole pair. The emission spectrum of the resulting ensemble consists mainly of a narrow band, 30–40 nm full width at half maximum and slightly Stokes-shifted with respect to the excitation band edge. Both excitation and emission depend on the nanocrystallite size. As a consequence, their optical properties are size-dependent and governed by quantum effects resulting in a quantization of energy levels reminiscent of that of single atoms or molecules.

Semiconductor QDs belong to either the elements combining from the II and VI groups, e.g., CdS, CdSe, CdTe or the elements combining from the III and V, e.g., GaAs, InP, InAs, etc. The main advantage offered by III–V semiconductor nanocrystals (as opposed to the II–VI QDs which are already commercially available) lies in the robustness of the covalent bond in III–V semiconductors vs. the ionic bond in the II–VI semiconductors, which might make them less cytotoxic [120]. So far, InP or other III–V QDs have not been used for bioimaging because they are difficult to prepare on a competitive time scale, and their quantum efficiencies tend to be much lower.

In most of the cases, "naked" QDs are susceptible to photo-oxidation and, thus, they need to be capped by a protective shell of an insulating material or wide-bandgap semiconductor structurally matched with the core material. The shell of QDs plays an important role. The shell should be transparent, be of non-emissive/higher band gap, and structurally similar to the core material so as to efficiently confine the excitation to the core. For instance, encapsulation of CdSe core by ZnS shell reduces the photochemical bleaching and dramatically increases its quantum yield [121]. Initially, chemically synthesized QDs could not be employed for biochemical applications because they did not disperse well in water, e.g., ZnS or TOPO (trioctylphosphine oxide)-coated QDs are hydrophobic in nature. It is, thus, necessary to make them "water soluble" (i.e., disperse them well in water) to facilitate their conjugation to biomolecules and make them useful for biological imaging. Some of the methods to make the QDs

water-dispersible are (i) derivatizing their surface with mercaptoacetic acid [111]; (ii) encapsulating them in phospholipid micelles [122]; (iii) derivatizing their surface with silica overcoat [123]; and (iv) coating them with an amine-modified poly(acrylic acid) [124,125]. Since hydrophilic surface treatment of QD was developed, the application range of QDs has been rapidly widening to bioimaging [111,126]. Correa-Duarte et al. [127] have reported that a silica coating leads to a 100-fold reduction in photo-corrosion rates for CdS nanoparticles. In our research group, water-dispersible silica-overcoated, highly luminescent and photostable (CdS:Mn/ZnS) (Fig. 4) semiconductor QDs have been prepared using the reverse micellar approach [128].

2.2.2.2.2. Properties. Some apparent advantages of using QDs over fluorescent dyes/probes are outlined below:
2.2.2.2.2.1. Spectral properties

(i) The emission spectra of QDs can be tuned across a wide range by changing the size and composition of the QD core, e.g., from UV-blue (ZnS [129]) to near-infrared (CdS/HgS/CdS [130], InP, InAs [131]) through the visible (CdE, with E = S, Se, Te [132]). Due to the importance of probes with excitation and emission in the NIR region (discussed earlier), focus on QDs emitting in the same region has been growing.

(ii) The excitation and emission spectra of the QDs are very favorable for biological detection. For instance, their broad excitation spectra and narrow emission spectra help in reduced spectral overlap, which improves the possibility of distinguishing multiple fluorophores simultaneously. In addition, the broad excitation spectra of QDs facilitate the use of a single excitation wavelength to excite QDs of different colors. These properties place QDs at an advantage over organic dyes, which have a narrow excitation and broad emission spectra.

Fig. 4. Bright yellow emission from CdS:Mn/ZnS QDs (right) and deionized water (left) as control. Reprinted by permission from (Ref. [28]), Copyright (2005) American Chemical Society.

2.2.2.2.2.2. Resistance to photobleaching. Photobleaching is a process in which molecular structure of a dye is irreversibly altered as a result of absorption of excitation light and renders it non-fluorescent. The photostable nature of the QD results from the shell surrounding the core. For example, capping the QD core with a large band gap semiconductor shell has been used to stabilize the core in the II–VI materials. It is found that, even under the high fluence of the confocal microscopy, the QDs fluorescence die down at a very slow rate [92]. In other cases, e.g., for III–V nanocrystals, the metastablility of surface capping agents is known to affect the electron-hole recombination. To take care of detrimental interfacial defects (which are formed due to strain developed during the growth stage), it is pointed out that the core and shell interfaces should be lattice mismatched [133,134]. Thus, for example, InAs cores have been covered by different shells made of ZnS, ZnSe, GaAs [133], etc.

2.2.2.2.2.3. Resistance to metabolic degradation. The inorganic nature of QDs and their passivating coatings help in their resistance to metabolic degradation. Jaiswal et al. [92] performed a cAMP-based starvation assay to check for any deleterious effects on cell viability and development and observed that cells loaded with QDs remained viable for more than 12 days. To study the toxicity of the QDs, Dubertret et al. [122] microinjected micelle-coated QDs into frog embryos, a delicate test system and tracked QDs up to tadpole stage. No explicit signs of any atypical phenotypes were observed at the end of the experiment. In vivo studies by Ballou et al. have also demonstrated the non-toxic nature of stably protected QDs [135].

2.2.2.2.2.4. High extinction coefficients. QDs have very large molar extinction coefficients and high quantum yields resulting in bright fluorescent probes [72]. Their molar extinction coefficients are of the order of $0.5–5 \times 10^{-6}$ M^{-1} cm^{-1} [136], which makes them bright probes in aqueous solutions [111] and also under photon-limited in vivo conditions (where light intensities are severely attenuated by scattering and absorption). Moreover, QDs have long fluorescence lifetimes on the order of 20–50 ns, which allows them to be distinguished from background and other fluorophores for increased sensitivity of detection [73]. Their high quantum yields (e.g., up to 85% [137]) are not significantly affected upon conjugation with proteins.

2.2.2.2.2.5. Conjugation ability. Bioconjugation of QDs can be achieved using several approaches, e.g., they can be conjugated to the linker [138] (e.g., avidin, protein A or protein G, or a secondary antibody) by covalent binding [122,139], passive adsorption, multivalent chelation or by electrostatic interactions. Since most proteins contain primary amine and carboxylic acid functional groups, carbodiimide-mediated amide formation cross-linking reactions are perhaps the most common as it obviates the need for any surface modification before conjugation. In the electrstatic self-assembly approach, the linker is fused to a positively charged peptide which enables it to be conjugated to dihydroxylipoic acid-capped zinc sulfide-coated QDs [132,138,140].

2.2.2.3. Gold nanoparticles

2.2.2.3.1. Basis of optical detection. Although nanosize metals like gold and silver do not fluoresce, they can provide colorimetric contrast induced by surface plasmon resonance (SPR). SPR can provide frequency dependent light absorption (color appearance) resulting from the collective oscillation of the conduction electrons induced by the incident electric field. Absorption bands appear when the incident photon frequency is in resonance with the collective excitation of the conductive electrons of the particle. Depending on particle size, shape and agglomeration, gold colloids can appear red, violet or blue as explained by the Mie scattering theory [141,142]. A 5-nm diameter gold particle has an absorption cross section more than 2 orders of magnitude higher than that of organic fluorophores [143–148] at room temperature. Usually, stable gold colloids (~15 nm) with small particle diameters and no agglomeration are red due to a narrow surface plasmon absorption band centered at 520 nm in their UV–vis spectrum. Any color change to violet or blue, corresponding to a characteristic red shift in the surface plasmon resonance of the particles from 520 to 574 nm, indicates agglomeration and subsequently, in many cases, particle precipitation [149]. Using a specific DNA target as a linking molecule to aggregate gold colloids with complementary probe sequences allows one to take advantage of the novel optical properties of dispersed versus aggregated gold particles for use in DNA detection [150–152].

2.2.2.3.2. Properties. The SPR frequency of gold nanoparticles depends on a number of factors, such as particle size [153–155], shape [156–158], solvent and ligand [159], dielectric properties [160,161], aggregate morphology [143,162–164], surface functionalization [165,166] and the refractive index of the surrounding medium [167–172]. Due to their unique optical (colorimetric) properties, gold nanoparticles are now finding increased applications in the detection of biological systems [143–148]. The optical properties of gold nanoparticles have been exploited for applications such as hybridization assays, DNA sequencing [173], detection of genetic disorders [147,174], immunoblotting, flow cytometry, etc. It seems possible to use specific organic moieties to fabricate and design nanoparticle aggregates whose spectra are sensitive to particle arrangement [162,175,176]. West's group [160,177] has prepared metal nanoshells consisting of a dielectric core (silica) with a metallic shell (gold) of nanometer thickness. They have shown that the optical resonance can be tuned in a controlled manner by varying the relative dimensions of the core and shell across the visible and into the infrared region of the spectrum. It is also implied that a nanoshell is over 1 million fold more likely than the comparable dye (indocyanine green) to encounter an absorbing event and convert that light into thermal energy [178]. By using NIR light and nanoshells, localized, irreversible photothermal ablation of tumor tissue both in vitro and in vivo was carried out under MRI guidance [178]. These nanoshells have also been used to develop a rapid immunoassay with sub-nanometer/milliliter sensitivity that can be performed on whole blood [179].

Colloidal gold offers some unique features over other labeling agents, e.g., QDs, organic dyes. For instance, it does not undergo any photodecomposition (and largely retains its optical properties; however, they may vary depending upon the medium surrounding it as discussed above), which is a common problem encountered

while using fluorescent dyes. Secondly, they are not apparently toxic, in sharp contrast to potential toxicity of semiconductor QDs. Third, they are reasonably stable and can be stored in dry state also. Lastly, their ability to shift the SPR, in a controlled fashion, to the spectral region best suited for optical bioimaging and biosensing applications would open the way to numerous additional bioapplications [180].

3. Design of nanoparticles for bioimaging application

The main parameters that need to be considered for the synthesis of nanoparticles for bioimaging applications are:

(i) Synthesis of optical core: The first step is the synthesis of the core, which encapsulates the fluorochrome, e.g., the dyes or the QDs. The most popular microemulsion system for preparation of nanoparticle is a "water-in-oil" (w/o) microemulsion system, and also commonly referred to as reverse micelles. W/o microemulsions have tremendous scope for manipulation of reaction conditions (i.e., by changing the surfactant co-surfactant, combination of surfactants and co-surfactants, composition and amount of polar media, oil, temperature, etc.) to suit the nanoparticle design. The reader may refer to some books which exhaustively cover this topic [181–184].

(ii) Synthesis of shell: The shell serves the purposes of protecting the optical core from the external environment thus improving its photostability (e.g., for organic dyes), enhancing the optical properties (by providing a lattice mismatch, e.g., for QDs) and providing further ability to bind/adhere to molecules for surface stability and bioconjugation.

(iii) Surface modification: There is a natural tendency for the particles to coagulate and aggregate. However, it is important that the nanoparticles remain suitably dispersed, preferably, in an aqueous environment for any application. This may be achieved by modifying the surface of the metal nanoparticles by employing various dispersing agents, e.g., surfactants, polymers, chelating groups, etc.

(iv) Bioconjugation and targeting: For targeted delivery of the nanoparticles to the desired site of action and binding, it is necessary to attach suitable biomolecules on the surface of the nanoparticles such as antibodies, peptides, enzymes, etc. These molecules can also act to promote or maintain their dispersion. The conjugation of nanoparticles and drugs, by passive (accumulation of drug or drug carrier system at a particular site due to physicochemical or pharmacological factors) and active targeting (specific modification of a nanosystems carrier with "agents" having selective affinity for recognition and interaction with specific cell, tissue [185], etc.) for various applications has been described by other investigators in detail [186,187].

All of the factors need to be considered concurrently in most cases to design optimum nanoparticulate systems for bioapplications such as in optical imaging. This is illustrated by the following examples of preparing the dye-doped organically modified silica nanoparticles, QDs and gold nanoparticles for bioimaging.

3.1. Dye-doped silica nanoparticles

(i) Optical core: Traditionally, silica nanoparticles have been prepared either by using a microemulsion mediated method [188–192] or the sol gel process [193–195] (i.e., Stober's method [196]). While in a typical Stober's method, alkoxysilane compounds (e.g., tetraethylorthosilicate (TEOS), tetramethylorthosilicate (TMOS) and their derivatives etc.) undergo base-catalyzed hydrolysis and condensation reaction in ammonia–ethanol–water mixture, similar reaction can takes place in the nanocores of the microemulsion system. In the case of dye-doped silica nanoparticles, the dye is encapsulated within a silica shell. Dye encapsulation is achieved by either covalent attachment of the dye with silica precursors [103,108,197,198] (e.g., with 3-(aminopropyl)triethoxysilane, APTS) before the hydrolysis in Stober's method or by first solubilising the dye in the core of the microemulsion and then carrying out the polymerization [15,97,199]. The advantage of using Stober's method is that the reaction can be scaled up easily to yield large amounts of nanoparticles, but the particle size may not be uniform and, moreover, different modifications of the particle surface are not easily achieved. Using a microemulsion method, fairly uniform sized nanoparticles can be prepared but the yields are extremely low. Importantly, the microemulsion-mediated method allows easy modulation of the nanoparticle surfaces for various applications.

(ii) Shell synthesis: The most common method is to use the microemulsion route to coat the core by carrying out further condensation of the silane reagents, i.e., TMOS/TEOS.

(iii) Surface modification: In order to allow for bioconjugation, the shell formation is done using either the amine derivative (e.g., APTS) or the carboxyl derivative. Other compounds can be introduced at this stage to obtain a better dispersion (prevent agglomeration) of the nanoparticles in the aqueous medium. For instance, TEOS, APTS and 3-(trihydroxysilyl)propylmethylphosphonate are added in controlled amounts to obtain good aqueous dispersions [15]. A schematic representation of the dye-doped and amine derivatized silica nanoparticle is shown in Fig. 5.
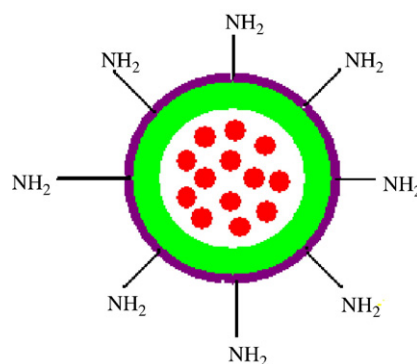

Fig. 5. (●) Dye-doped silica particles; (◉) surface functionalized with amine groups for bioconjugation.

(iv) Bioconjugation: Most biomolecules, such as proteins, contain primary amine and carboxylic groups which can be covalently attached to the carboxyl functionalized nanoparticle, using carbodiimide-coupling chemistry [200].

He et al. have developed a fluorescent labeling method based on biological fluorescent nanoparticles [99] using dye-doped fluorescent silica nanoparticles. The particles prepared by the w/o microemulsion method are covalently immobilized with anti-human liver cancer monoclonal antibody HAb18 (to recognize HepG liver cancer cells) and can identify the target cells selectively and efficiently. Dye-labeled particles can also be used in quantitative real-space studies with confocal fluorescence microscopy, time-resolved phosphorescence anisotropy [201]. They can be used also as photostable biomarkers [96–98], biosensors [102,202] and DNA hybridization analysis [203] cancer cell recognition [99], including fluorescent-linked immunosorbent assay, immunocytochem, immunohistochem [100], etc. By combining the high-intensity luminescent nanoparticles with the specifity of antibody-mediated recognition, ultrasensitive target detection has been achieved in various fluorescence labeling techniques, including DNA microarray and protein microarray [100]. In a similar way, spherical nanosized luminol/ SiO_2 composite particles synthesized using reverse micelles were modified with chitosan and used to label DNA [203].

Our group has recently prepared multimodal nanoparticles containing gadolinium and dye (i.e., tris(2,2′-bipyridyl)dichloruthenium(II)hexahydrate: Rubpy)-doped silica (Rubpy:Gd^{III}/ SiO_2) nanoparticles which can be readily bioconjugated. While the dye encapsulated in the core of the nanoparticle provided the optical detection capability, Gd^{III} chelated to the surface of the nanoparticles using silane ligands enabled MR sensitivity. In order to demonstrate multimodal imaging capability, Rubpy: Gd^{III}/SiO_2 nanoparticles were first conjugated to folate and then incubated with human lung cancer cells (A-549) [204]. Fig. 6 shows the fluorescence and MRI images of the gel, which clearly show effective loading of nanoparticles into A-549 cells and multimodal bioimaging capability of these nanoparticles. Both inorganic (e.g., Rubpy) [15,97] as well as organic(tetramethylrhodamine) [101] dyes can be incorporated in the silica matrix with suitable modification. In a recent example, a combination of dyes (tris(2,2′-bipyridyl)osmium(II)bis(hexafluorophosphate) and Rubpy) was simultaneously entrapped inside silica nanoparticles at precisely controlled ratios. The single-wavelength excitation with dual emission endowed the nanoparticles with an optical encoding capability for rapid and high-throughput multiplexed detection [205]. Furthermore, Tan's group has also prepared silica nanoparticles encapsulated with three dyes. They have shown that, by varying the doping ratio, the fluorescence resonance energy transfer-mediated emission signatures can be tuned such that the nanoparticles exhibit multiple colors under one single wavelength excitation [199].

3.2. Quantum dots

(i) Optical core synthesis: The subject of semiconductor nanoparticle preparation and properties has been covered in previous reviews [206–210]. In the past, QDs have been prepared by precipitation of the metal, e.g., Hg, Zn, Cd with the hydroxide of S, Se, etc. in the presence of the colloidal stabilizers [211,212]. A recent and more commonly used method involves high temperature (300 °C), surfactant synthesis starting from dimethyl-cadmium precursors in TOPO or hexadecyl amine. This hot synthesis method yields highly crystalline QDs with high quantum yields. The surfactant covers the growing crystallites and prevents their aggregation, as well as limits the dissolution of smaller nanocrystals in favor of larger ones (a process known as Ostwald ripening). Another method used frequently for QDs preparation is the w/o microemulsion (reverse micellar) method. Here the precipitation between the metal and the chalcogenide is carried out in the water domain of the reverse micelle, which yields surfactant-capped nanocrystals. CdS [213–215] CdS/ZnS [216], CdSe [217], CdMnS [218,219], ZnSe [220], ZnS:Mn [221], ZnS:Mn/ZnS [222], etc., QDs have been prepared using w/o microemulsions.

(ii) Shell synthesis: The core is covered with a shell of a large band gap semiconductor shell (for reasons discussed above under "resistance to photobleaching"). For example, in the CdSe core QDs are covered by the epitaxially matched ZnS layer, which effectively passivates the surface defects of CdSe, prevents photo-corrosion and thus improves the
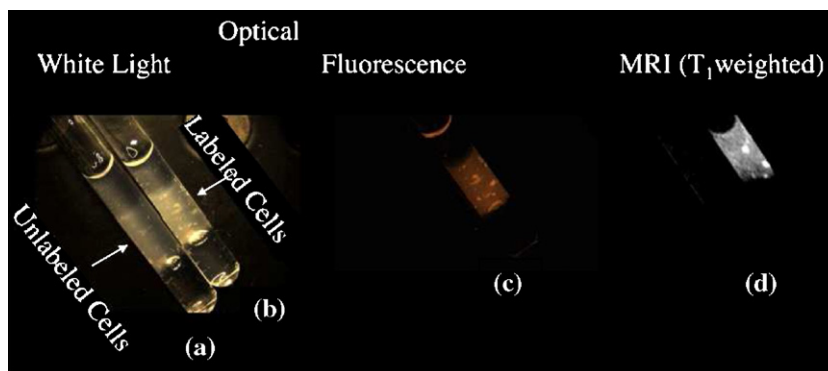

Fig. 6. Cancer cell imaging using multimodal nanoparticles. (a) 1×10^{-6} A549 cells in 2% agarose; (b) nanoparticles labeled cells visualized under white light illumination; (c) labeled cells visualized using reflectance fluorescence imaging; and (d) labeled cells detected by MRI on T_1 weighted scans. Reprinted by permission from Adenine Press (Ref. [204]), Copyright (2005).

quantum yield. Similarly, capping has also been achieved using ZnSe [223]. The shell formation is carried out subsequent to the formation of the QD core. In our group, Santra et al. have recently prepared highly luminescent and photostable CdS: Mn/ZnS core/shell QDs [110,128].

(iii) Surface modification: The nanocrystals formed using TOPO are capped with a monolayer of the organic ligand and are soluble only in non-polar solvents. For bioimaging applications, these hydrophobic dots can be made water dispersible by using amphiphilic polymers such as poly(ethylene glycol)(PEG). Other polymers used include poly(acrylic acid), PEG-derivatized phospholipids, block copolymers and polyanhydrides [122,224,225]. PEG not only enhances the aqueous solubility of the QDs but also reduces nonspecific adhesion to biological cells. Pegylation has proven to be fully compatible with QD surface chemistries and is bound to play a prevalent role when optimizing in vivo pharmacokinetics of QD bio-probes [135]. The surface of the QDs has also been protected by silica layer [123].

(iv) Bioconjugation: All QDs surface chemistries are designed to provide reactive groups such as amine ($-NH_2$), carboxyl ($-COOH$) or mercapto ($-SH$) groups for direct conjugation to biomolecules. Finally, the QDs are conjugated to the linker (e.g., avidin, protein A or protein G, or a secondary antibody) by covalent binding passive adsorption, multivalent chelation or by electrostatic interactions (discussed above, under conjugation ability).

Some recent reviews have dwelled on the applications of QDs as bio-probes [226–229]. The potential benefits of the use of conjugated QD probes to monitor cellular functions has prompted extensive efforts to develop methods for synthesizing water-dispersible and biocompatible QDs that can be widely used for fluorescent-based bioimaging [225,230,231]. QDs have been used to image blood vessel [232], to target tissue-specific vascular markers [233] and to image lymph nodes [79] in mice. QDs are, thus, highly suited for imaging cells deep within tissues[79,232,234,235].

3.3. Gold nanoparticles

(i) Optical core synthesis: As described earlier, nanosize gold provides colorimetric contrast induced by surface plasmon resonance (SPR), which is a function of the size, shape and dielectric constant of the medium. A large number of methods, which give control over the above parameters, are used to prepare gold nanoparticles. The common methods include reduction of gold precursors in the presence of capping agents [155,236], by the use of microemulsions [237–239], copolymer micelles [240], reversed micelles [239], surfactant, membranes, by the seed mediated method [241], reduction of gold precursors using a combination of appropriate reducing agents and radiation such as ultrasound [242–247], heat [248–250], etc.

(ii) Surface modification. It is necessary to modify the gold nanoparticle surface to improve its dispersion and also to allow for bio-conjugation for imaging applications. Liu and Han report an efficient process for preparing monodisperse SiO_2-coated Au nanoparticles using vigorous shaking (rather than magnetic stirring) and without the use of surface-coupling silane agents or large stabilizers [251]. Recently, chitosan has been used as a reducing and stabilizing agent for gold nanoparticles [252].

(iii) Bioconjugation: The positively charged protein can be conjugated to negatively charged gold nanoparticles via electrostatic interactions [253], or by chemical bond formation between protein molecules containing sulpho-hydryl ($-SH$) groups which have high affinity towards the gold atoms. Mirkin's group demonstrated in 1997 that gold nanoparticles could be surface functionalized with thiolated oligonucleotides and stabilized in aqueous biological buffers [143].

Different groups [174,254] have shown that it is possible to detect a wide range of biological macromolecules using modified gold nanoparticles offering distinct 'Raman Signatures'. It is now known that only a very small number of molecules, located in the gap between two nearly touching gold nanocrystals on the surface, actually provide the enhanced signal [255]. Gold nanoparticle bioconjugates have been applied to polynucleotide detection using mercaptoalkyl oligonucleotide-modified gold nanoparticle by exploiting the change in optical properties resulting from plasmon–plasmon interactions between locally adjacent gold nanoparticles [143]. Gold nanoshells have also been fabricated for near-IR resonance, and antibodies against target antigens were conjugated to the nanoshell surfaces [179]. When introduced into samples containing the appropriate antigen, the antibody–antigen linkage caused the gold nanoshells to aggregate, shifting the resonant wavelength further into the IR. In addition, due to excellent biocompatibility [256–258] and available facile bioconjugation protocols [259] (e.g., to attach proteins), gold nanoparticles have also been used for tumor directed drug delivery [260,261]. Gold nanoparticles resistance to photodecomposition, SPR tuning capability and non-toxic nature provide it some unique advantages over other conventional probes.

4. Trends and opportunities

Fluorescence is a widely used tool in biology. The drive to measure more biological processes simultaneously imposes new demands on the fluorescent probes used in these experiments.

While there has been much progress in molecular imaging with nuclear techniques (PET, SPECT, etc.) fluorescent probes, and now, particularly, near-IR fluorochromes, coupled with fluorescence-enhanced tomography may offer greater imaging sensitivity owing to the repeated activation, relaxation and re-emission of fluorescent photons by the NIR fluorophores. However, many of these organic dyes are hydrophobic and/or their fluorescence is quenched in isotonic conditions. Nanoparticle technology has been utilized to overcome the hydrophobic property of these dyes, but problems still remain in their fabrication.

Some critical aspects that need to be addressed before these (fluorophores) can be employed for clinical translation are:

(i) Detection of the fluorescent signals generated from deeply located targets at the tissue surface;

(ii) Optimization of loading of encapsulated dye for optimum detection;

(iii) Sufficient photostability for in vivo applications;

(iv) Synthesis of a range of NIR dyes, with fluorescence in the NIR window, 650–900 nm, for application to varied biological samples; and

(v) Ideal probes for multicolor experiments should have a narrow symmetric emission spectrum (in contrast to conventional dyes with a broad emission spectrum with a long tail at red wavelengths), and the whole group of probes should be excitable at a single wavelength [262].

While QDs have emerged as promising probes for bioimaging, and particularly for multiplexing, there are a number of issues that warrant attention before their full potential can be realized. After coating (done to improve the dispersion in water and bioconjugation), the dimensions of a QDs approach those of large proteins (7–15 nm); this may limit access to parts of tumors. Moreover, the semiconductor crystallites are relatively dense (specific gravity 5–6) and massive ($\sim$ 500 kDa); it is possible that they may affect labeling in vivo. Another negative photophysical aspect of these particles has been fluorescence intermittency (blinking) [263]. Many researchers have shown that there is no, or small, toxicity linked to such particles [92,122] but there have been other reports in the literature about their toxicity. In fact, a widespread replacement of organic fluorophores with II/ VI type QDs in bioimaging is hindered by the inherent cytotoxicity of the individual ions (Cd^{2+}, Se^{2+} and Te^{2+}) that the QDs are composed of [264,265]. Yamazaki et al. have found InP to be comparatively less toxic [266]. This makes III–V QDs potentially better candidates than II–VI QDs (e.g., CdSe) for biological applications such as bioimaging and photodynamic therapy.

Acknowledgement

References

[1] Murray CB, Kagan CR, Bawendi MG. Annu Rev Mater Sci 2000;30:545.
[2] Hochella MF. Earth Planet Sci Lett 2002;203:593.
[3] Roco MC, Bainbridge WS. J Nanopart Res 2005;7:1.
[4] Mazzola L. Nat Biotechnol 2003;21:1137.
[5] Paull R, Wolfe J, Hebert P, Sinkula M. Nat Biotechnol 2003;21:1144.
[6] Micro and Nanotechnology Commercialization Education Foundation, Roadmap 2nd Edition, 2004 (http://www.mancef.org/).
[7] http://www.biotechsystems.com.
[8] Mahmood U. IEEE Eng Med Biol Mag 2004;23:58.
[9] Pomper MG, Hammoud DA. IEEE Eng Med Biol Mag 2004;23:28.
[10] Hogemann D, Basilion JP. Eur J Nucl Med Mol Imaging 2002;29:400.
[11] Hogemann D, Basilion JP, Weissleder R. Radiologe 2001;41:116.
[12] Bremer C, Ntziachristos V, Mahmood U, Tung CH, Weissleder R. Radiologe 2001;41:131.
[13] Mahmood U, Weissleder R. Acad Radiol 2002;9:629.
[14] Kircher MF, Mahmood U, King RS, Weissleder R, Josephson L. Cancer Res 2003;63:8122.
[15] Santra S, Bagwe RP, Dutta D, Stanley JT, Walter GA, Tan W, et al. Adv Mater 2005;17:2165.
[16] Kayyem JF, Kumar RM, Fraser SE, Meade TJ. Chem Biol 1995;2:615.
[17] Liang ZP, Lauterbur PC. IEEE Trans Med Imaging 1994;13:677.
[18] Moats RA, Fraser SE, Meade TJ. Angew Chem Int Ed Engl 1997;36:726.
[19] Merbach AE, v. T*th. The chemistry of contrast agents in medical magnetic resonance imaging. Chichester, New York: Wiley; 2001.
[20] Demos SG, Radousky HB, Alfano RR. Opt Express 2000;7:23.
[21] Dunn AK, Bolay T, Moskowitz MA, Boas DA. J Cereb Blood Flow Metab 2001;21:195.
[22] Tearney GJ, Brezinski ME, Bouma BE, Boppart SA, Pitris C, Southern JF, et al. Science 1997;276:2037.
[23] Weissleder R, Ntziachristos V. Nat Med 2003;9:123.
[24] Ntziachristos V, Ripoll J, Wang LHV, Weissleder R. Nat Biotechnol 2005;23:313.
[25] Rudin M, Weissleder R. Nat Rev Drug Discov 2003;2:123.
[26] Licha K, Olbrich C. Adv Drug Deliv Rev 2005;57:1087.
[27] Alivisatos P. Nat Biotechnol 2004;22:47.
[28] Weissleder R, Mahmood U. Radiology 2001;219:316.
[29] Pomper MG. Acad Radiol 2001;8:1141.
[30] Licha K, Hessenius C, Becker A, Henklein P, Bauer M, Wisniewski S, et al. Bioconjug Chem 2001;12:44.
[31] Weissleder R. Nat Biotechnol 2001;19:316.
[32] Ntziachristos V, Schellenberger EA, Ripoll J, Yessayan D, Graves E, Bogdanov Jr A, et al. Proc Natl Acad Sci U S A 2004;101:12294.
[33] Graves EE, Culver JP, Ripoll J, Weissleder R, Ntziachristos V. J Opt Soc Am A Opt Image Sci Vis 2004;21:231.
[34] Graves EE, Yessayan D, Turner G, Weissleder R, Ntziachristos V. J Biomed Opt 2005;10:44019.
[35] Graves EE, Ripoll J, Weissleder R, Ntziachristos V. Med Phys 2003;30:901.
[36] Graves EE, Weissleder R, Ntziachristos V. Curr Mol Med 2004;4:419.
[37] Ntziachristos V, Bremer C, Tung C, Weissleder R. Acad Radiol 2002;9:S323.
[38] Ntziachristos V, Weissleder R. Med Phys 2002;29:803.
[39] Gao M, Lewis G, Turner GM, Soubret A, Ntziachristos V. Appl Opt 2005;44:5468.
[40] Gremlich HU, Martinez V, Kneuer R, Kinzy W, Weber E, Pfannkuche HJ, et al. Mol Imaging 2004;3:303.
[41] Tung CH, Quinti L, Jaffer FA, Weissleder R. Mol Pharm 2005;2:92.
[42] Wunder A, Schellenberger E, Mahmood U, Bogdanov Jr A, Muller-Ladner U, Weissleder R, et al. Mol Imaging 2005;4:1.
[43] Ntziachristos V, Bremer C, Graves EE, Ripoll J, Weissleder R. Mol Imaging 2002;1:82.
[44] Bremer C, Ntziachristos V, Weitkamp B, Theilmeier G, Heindel W, Weissleder R. Invest Radiol 2005;40:321.
[45] Jain RK, Munn LL, Fukumura D. Nat Rev Cancer 2002;2:266.
[46] Tozer GM, Ameer-Beg SM, Baker J, Barber PR, Hill SA, Hodgkiss RJ, et al. Adv Drug Deliv Rev 2005;57:135.
[47] Sumen C, Mempel TR, Mazo IB, von Andrian UH. Immunity 2004;21:315.
[48] Gavins FN, Chatterjee BE. J Pharmacol Toxicol Methods 2004;49:1.
[49] Hudetz AG. Microcirculation 1997;4:233.
[50] Labas YA, Gurskaya NG, Yanushevich YG, Fradkov AF, Lukyanov KA, Lukyanov SA, et al. Proc Natl Acad Sci U S A 2002;99:4256.
[51] Gurskaya NG, Fradkov AF, Terskikh A, Matz MV, Labas YA, Martynov VI, et al. FEBS Lett 2001;507:16.
[52] Peyker A, Rocks O, Bastiaens PIH. Chembiochem 2005;6:78.
[53] Lukyanov KA, Chudakov DM, Lukyanov S, Verkhusha VV. Nat Rev Mol Cell Biol 2005;6:885.

[54] Yanushevich YG, Shagin DA, Fradkov AF, Shakhbazov KS, Barsova EV, Gurskaya NG, et al. Russ J Bioorgan Chem 2005;31:43.

[55] Demidova TN, Gad F, Zahra T, Francis KP, Hamblin MR. J Photochem Photobiol B Biol 2005;81:15.

[56] Burch S, Bisland SK, Bogaards A, Yee AJM, Whyne CM, Finkelstein JA, et al. J Orthop Res 2005;23:995.

[57] Gade TP, Hassen W, Santos E, Gunset G, Saudemont A, Gong MC, et al. Cancer Res 2005;65:9080.

[58] Smith PG, Oakley F, Fernandez M, Mann DA, Lemoine NR, Whitehouse A. Gene Ther 2005;12:1465.

[59] Zhao H, Doyle TC, Coquoz O, Kalish F, Rice BW, Contag CH. J Biomed Opt 2005;10.

[60] Villalobos C, Nadal A, Nunez L, Quesada I, Chamero P, Alonso MT, et al. Cell Calcium 2005;38:131.

[61] Roda A, Guardigli M, Pasini P, Mirasoli M, Michelini E, Musiani M. Anal Chim Acta 2005;541:25.

[62] Shah K, Tung CH, Breakefield XO, Weissleder R. Molec Ther 2005;11:926.

[63] Heine HL, Leong HS, Rossi FM, McManus BM, Podor TJ. Methods Mol Med 2005;112:109.

[64] Wang Y, Iyer M, Annala AJ, Chappell S, Mauro V, Gambhir SS. J Nucl Med 2005;46:667.

[65] Hoffman RM. Lancet Oncol 2002;3:546.

[66] Matz MV, Lukyanov KA, Lukyanov SA. Bioessays 2002;24:953.

[67] Hoffman RM. Methods Mol Med 2005;111:297.

[68] Terakawa S. Tanpakushitsu Kakusan Koso 2004;49:1641.

[69] Tran PT, Paoletti A, Chang F. Methods 2004;33:220.

[70] Weston SA, Parish CR. J Immunol Methods 1990;133:87.

[71] Lyons AB, Parish CR. J Immunol Methods 1994;171:131.

[72] Chan WC, Maxwell DJ, Gao X, Bailey RE, Han M, Nie S. Curr Opin Biotechnol 2002;13:40.

[73] Bruchez Jr M, Moronne M, Gin P, Weiss S, Alivisatos AP. Science 1998;281:2013.

[74] Bornhop DJ, Contag CH, Licha K, Murphy CJ. J Biomed Opt 2001;6:106.

[75] Lin Y, Weissleder R, Tung CH. Mol Imaging 2003;2:87.

[76] Licha K, Riefke B, Ntziachristos V, Becker A, Chance B, Semmler W. Photochem Photobiol 2000;72:392.

[77] Pham W, Lai WF, Weissleder R, Tung CH. Bioconjug Chem 2003;14:1048.

[78] Frangioni JV. Curr Opin Chem Biol 2003;7:626.

[79] Kim S, Lim YT, Soltesz EG, De Grand, Lee J, Nakayama A, et al. Nat Biotechnol 2004;22:93.

[80] Weinmann HJ, Laniado M, Mutzel W. Physiol Chem Phys Med Nmr 1984;16:167.

[81] Ludemann L, Hamm B, Zimmer C. Magn Reson Imaging 2000;18:1201.

[82] Knauth M, Wirtz CR, Aras N, Sartor K. Neuroradiology 2001;43:254.

[83] Knauth M, Aras N, Wirtz CR, Dorfler A, Engelhorn T, Sartor K. Am J Neuroradiol 1999;20:1547.

[84] Shen T, Weissleder R, Papisov M, Bogdanov Jr A, Brady TJ. Magn Reson Med 1993;29:599.

[85] Weissleder R, Bogdanov A, Neuwelt EA, Papisov M. Adv Drug Deliv Rev 1995;16:321.

[86] Tiefenauer LX, Tschirky A, Kuhne G, Andres RY. Magn Reson Imaging 1996;14:391.

[87] Stark DD, Bradley WG. Magnetic resonance imaging. St. Louis: Mosby-Year Book; 1992.

[88] Gupta H, Weissleder R. Magn Reson Imaging Clin N Am 1996;4:171.

[89] Comblin V, Gilsoul D, Hermann M, Humblet V, Jacques V, Mesbahi M, et al. Coord Chem Rev 1999;186:451.

[90] Woods M, Botta M, Avedano S, Wang J, Sherry AD. Dalton Trans 2005;3829.

[91] Song LL, Hennink EJ, Young IT, Tanke HJ. Biophys J 1995;68:2588.

[92] Jaiswal JK, Mattoussi H, Mauro JM, Simon SM. Nat Biotechnol 2003;21:47.

[93] Zheng G, Li H, Yang K, Blessington D, Licha K, Lund-Katz S, et al. Bioorg Med Chem Lett 2002;12:1485.

[94] Ye YP, Li WP, Anderson CJ, Kao J, Nikiforovich GV, Achilefu S. J Am Chem Soc 2003;125:7766.

[95] Bagwe RP, Yang CY, Hilliard LR, Tan WH. Langmuir 2004;20:8336.

[96] Santra S, Zhang P, Wang KM, Tapec R, Tan WH. Anal Chem 2001;73:4988.

[97] Santra S, Wang KM, Tapec R, Tan WH. J Biomed Opt 2001;6:160.

[98] Santra S, Dutta D, Moudgil BM. Food Bioprod Process 2005;83:136.

[99] He XX, Duan JH, Wang KM, Tan WH, Lin X, He CM. J Nanosci Nanotechnol 2004;4:585.

[100] Lian W, Litherland SA, Badrane H, Tan WH, Wu DH, Baker HV, et al. Anal Biochem 2004;334:135.

[101] Zhao XJ, Bagwe RP, Tan WH. Adv Mater 2004;16:173.

[102] Tapec R, Zhao XJJ, Tan WH. J Nanosci Nanotechnol 2002;2:405.

[103] Santra S, Liesenfeld B, Bertolino C, Dutta D, Cao Z, Tan W, et al. J Lumin 2006;117:75.

[104] Rosi NL, Mirkin CA. Chem Rev 2005;105:1547.

[105] Smith PW. J Cell Biochem (Suppl) 2002;39:54.

[106] Velikov KP, van Blaaderen A. Langmuir 2001;17:4779.

[107] Vanblaaderen A, Vrij A. Langmuir 1992;8:2921.

[108] Qhobosheane M, Santra S, Zhang P, Tan WH. Analyst 2001;126:1274.

[109] Qhobosheane M, Zhang P, Tan W. J Nanosci Nanotechnol 2004;4:635.

[110] Santra S, Yang H, Stanley JT, Holloway PH, Moudgil BM, Walter G, et al. Chem Commun 2005;3144.

[111] Chan WC, Nie S. Science 1998;281:2016.

[112] Weller H. Adv Mater 1993;5:88.

[113] Steigerwald ML, Brus LE. Acc Chem Res 1990;23:183.

[114] Weller H. Angew Chem Int Ed Engl 1993;32:41.

[115] Alivisatos AP. J Phys Chem 1996;100:13226.

[116] Zhang JZ. Acc Chem Res 1997;30:423.

[117] Weller H. Curr Opin Colloid Interface Sci 1998;3:194.

[118] Empedocles S, Bawendi M. Acc Chem Res 1999;32:389.

[119] Gaponenko SV. Optical properties of semiconductor nanocrystals. Cambridge, UK: Cambridge Unviersity Press; 1998.

[120] Talapin DV, Gaponik N, Borchert H, Rogach AL, Haase M, Weller H. J Phys Chem B 2002;106:12659.

[121] Hines MA, Guyot-Sionnest P. J Phys Chem 1996;100:468.

[122] Dubertret B, Skourides P, Norris DJ, Noireaux V, Brivanlou AH, Libchaber A. Science 2002;298:1759.

[123] Yang HS, Holloway PH, Santra S. J Chem Phys 2004;121:7421.

[124] Wu XY, Liu HJ, Liu JQ, Haley KN, Treadway JA, Larson JP, et al. Nat Biotechnol 2003;21:452.

[125] Wu XY, Liu HJ, Liu JQ, Haley KN, Treadway JA, Larson JP, et al. Nat Biotechnol 2003;21:41.

[126] Goldman ER, Balighian ED, Mattoussi H, Kuno MK, Mauro JM, Tran PT, et al. J Am Chem Soc 2002;124:6378.

[127] Correa-Duarte MA, Giersig M, Liz-Marzan LM. Chem Phys Lett 1998;286:497.

[128] Santra S, Yang H, Holloway PH, Stanley JT, Mericle RA. J Am Chem Soc 2005;127:1656.

[129] Weller H, Koch U, Gutierrez M, Henglein A. Ber Bunsenges Phys Chem Chem Phys 1984;88:649.

[130] Eychmuller A, Mews A, Weller H. Chem Phys Lett 1993;208:59.

[131] Guzelian AA, Katari JEB, Kadavanich AV, Banin U, Hamad K, Juban E, et al. J Phys Chem 1996;100:7212.

[132] Mattoussi H, Mauro JM, Goldman ER, Anderson GP, Sundar VC, Mikulec FV, et al. J Am Chem Soc 2000;122:12142.

[133] Cao YW, Banin U. J Am Chem Soc 2000;122:9692.

[134] Micic OI, Smith BB, Nozik AJ. J Phys Chem B 2000;104:12149.

[135] Ballou B, Lagerholm BC, Ernst LA, Bruchez MP, Waggoner AS. Bioconjug Chem 2004;15:79.

[136] Leatherdale CA, Woo WK, Mikulec FV, Bawendi MG. J Phys Chem B 2002;106:7619.

[137] Peng ZA, Peng XG. J Am Chem Soc 2001;123:183.

[138] Goldman ER, Anderson GP, Tran PT, Mattoussi H, Charles PT, Mauro JM. Anal Chem 2002;74:841.

[139] Gerion D, Pinaud F, Williams SC, Parak WJ, Zanchet D, Weiss S, et al. J Phys Chem B 2001;105:8861.

[140] Medintz IL, Clapp AR, Mattoussi H, Goldman ER, Fisher B, Mauro JM. Nat Mater 2003;2:630.

[141] Feldheim DL, Foss CA. Metal Nanoparticles: Synthesis, Characterization, and Applications. New York: Marcel Dekker; 2002.

[142] Bohren CF, Huffman DR. Absorption and scattering of light by small particles. New York: Wiley; 1983.

[143] Elghanian R, Storhoff JJ, Mucic RC, Letsinger RL, Mirkin CA. Science 1997;277:1078.

[144] Storhoff JJ, Elghanian R, Mucic RC, Mirkin CA, Letsinger RL. J Am Chem Soc 1998;120:1959.

[145] Storhoff JJ, Lazarides AA, Mucic RC, Mirkin CA, Letsinger RL, Schatz GC. J Am Chem Soc 2000;122:4640.

[146] Reynolds RA, Mirkin CA, Letsinger RL. J Am Chem Soc 2000;122: 3795.

[147] Taton TA, Mirkin CA, Letsinger RL. Science 2000;289:1757.

[148] Cao YW, Jin R, Mirkin CA. J Am Chem Soc 2001;123:7961.

[149] Hayat MA. Colloidal Gold: Principles, Methods, and Applications. San Diego: Academic Press; 1989.

[150] He L, Musick MD, Nicewarner SR, Salinas FG, Benkovic SJ, Natan MJ, et al. J Am Chem Soc 2000;122:9071.

[151] Jin RC, Wu GS, Li Z, Mirkin CA, Schatz GC. J Am Chem Soc 2003;125:1643.

[152] Thaxton CS, Georganopoulou DG, Mirkin CA. Clin Chim Acta 2006;363:120.

[153] Khlebtsov NG, Trachuk LA, Mel'nikov AG. Opt Spectrosc 2005;98:77.

[154] Kreibig U, Genzel L. Surf Sci 1985;156:678.

[155] Turkevich J, Stevenson PC, Hillier J. Discuss Faraday Soc 1951:55.

[156] Sarkar D, Halas NJ. Phys Rev E 1997;56:1102.

[157] Murphy CJ, Jana NR. Adv Mater 2002;14:80.

[158] Jin RC, Cao YW, Mirkin CA, Kelly KL, Schatz GC, Zheng JG. Science 2001;294:1901.

[159] Ghosh SK, Nath S, Kundu S, Esumi K, Pal T. J Phys Chem B 2004;108:13963.

[160] Oldenburg SJ, Averitt RD, Westcott SL, Halas NJ. Chem Phys Lett 1998;288:243.

[161] Haynes CL, Van Duyne RP. J Phys Chem B 2001;105:5599.

[162] Novak JP, Feldheim DL. J Am Chem Soc 2000;122:3979.

[163] Novak JP, Nickerson C, Franzen S, Feldheim DL. Anal Chem 2001;73:5758.

[164] Brousseau LC, Novak JP, Marinakos SM, Feldheim DL. Adv Mater 1999;11:447.

[165] Caruso RA, Antonietti M. Chem Mater 2001;13:3272.

[166] Marinakos SM, Novak JP, Brousseau LC, House AB, Edeki EM, Feldhaus JC, et al. J Am Chem Soc 1999;121:8518.

[167] Malinsky MD, Kelly KL, Schatz GC, Van Duyne RP. J Am Chem Soc 2001;123:1471.

[168] Cocchini F, Bassani F, Bourg M. Surf Sci 1985;156:851.

[169] Mulvaney P, Liz-Marzan LM, Giersig M, Ung T. J Mater Chem 2000;10:1259.

[170] Underwood S, Mulvaney P. Langmuir 1994;10:3427.

[171] LizMarzan LM, Giersig M, Mulvaney P. Langmuir 1996;12:4329.

[172] Neeves AE, Birnboim MH. J Opt Soc Am B Opt Phys 1989;6:787.

[173] Mirkin CA, Letsinger RL, Mucic RC, Storhoff JJ. Nature 1996;382: 607.

[174] Cao YWC, Jin RC, Mirkin CA. Science 2002;297:1536.

[175] Zanchet D, Micheel CM, Parak WJ, Gerion D, Alivisatos AP. Nano Lett 2001;1:32.

[176] Loweth CJ, Caldwell WB, Peng XG, Alivisatos AP, Schultz PG. Angew Chem Int Ed Engl 1999;38:1808.

[177] Averitt RD, Westcott SL, Halas NJ. J Opt Soc Am B Opt Phys 1999;16:1824.

[178] Hirsch LR, Stafford RJ, Bankson JA, Sershen SR, Rivera B, Price RE, et al. Proc Natl Acad Sci U S A 2003;100:13549.

[179] Hirsch LR, Jackson JB, Lee A, Halas NJ, West J. Anal Chem 2003;75:2377.

[180] Lim YT, Park OO, Jung HT. J Colloid Interface Sci 2003;263:449.

[181] Mittal KL, Kumar P. Handbook of microemulsion science and technology. New York: Marcel Dekker; 1999.

[182] Pileni MP. Structure and reactivity in reverse micelles. Amsterdam: Elsevier; 1989.

[183] Rosano HL, Clausse M. Microemulsion systems. New York, N.Y.: M. Dekker; 1987.

[184] Fendler JH. Membrane mimetic chemistry: characterizations and applications of micelles, microemulsions, monolayers, bilayers, vesicles, host–guest systems, and polyions. New York: Wiley; 1982.

[185] Nishioka Y, Yoshino H. Adv Drug Deliv Rev 2001;47:55.

[186] Vasir JK, Reddy MK, Labhasetwar VD. Curr Nanosci 2005;1:47.

[187] Garnett MC. Adv Drug Deliv Rev 2001;53:171.

[188] Arriagada FJ, Osseoasare K. J Colloid Interface Sci 1995;170:8.

[189] Arriagada FJ, Osseoasare K. J Dispers Sci Technol 1994;15:59.

[190] Arriagada FJ, Osseoasare K. Colloids Surf 1992;69:105.

[191] Arriagada FJ, Osseo-Asare K. J Colloid Interface Sci 1999;211:210.

[192] Osseoasare K, Arriagada FJ. Colloids Surf 1990;50:321.

[193] Klein LC. Sol–gel technology for thin films, fibers, preforms, electronics, and specialty shapes. Park Ridge, N.J.: Noyes Publications; 1988.

[194] Schmidt H. J Non-Cryst Solids 1988;100:51.

[195] Ulrich DR. J Non-Cryst Solids 1988;100:174.

[196] Stober W, Fink A, Bohn E. J Colloid Interface Sci 1968;26:62.

[197] Santra S, Yang H, Dutta D, Stanley JT, Holloway PH, Tan WH, et al. Chem Commun 2004:2810.

[198] Santra S, Liesenfeld B, Dutta D, Chatel D, Batich CD, Tan WH, et al. J Nanosci Nanotechnol 2005;5:899.

[199] Wang L, Tan WH. Nano Lett 2006;6:84.

[200] Wang S, Low PS. J Control Release 1998;53:39.

[201] Lettinga MP, van Zandvoort MAMJ, van Kats CM, Philipse AP. Langmuir 2000;16:6156.

[202] Senarath-Yapa MD, Saavedra SS, Aspinwall CA, Roberts DL. Abstr Pap Am Chem Soc 2004;227:U849.

[203] Qian KJ, Zhang L, Yang ML, He PG, Fang YZ. Chin J Chem 2004;22:702.

[204] Santra S, Dutta D, Walter GA, Moudgil BM. Technol Cancer Res Treat 2005;4:593.

[205] Wang L, Yang C, Tan W. Nano Lett 2005;5:37.

[206] Green M. Chem Commun 2005:3002.

[207] Green M. Curr Opin Solid State Mater Sci 2002;6:355.

[208] Green M, O'Brien P. Chem Commun 1999:2235.

[209] Kelly JM, O'Brien P, Weller H, Green M, Harding JH. Philos Trans R Soc Lond Ser A Math Phys Eng Sci 2003;361:310.

[210] Grieve K, Mulvaney P, Grieser F. Curr Opin Colloid Interface Sci 2000;5:168.

[211] Duonghong D, Ramsden J, Gratzel M. J Am Chem Soc 1982;104:2977.

[212] Rossetti R, Brus L. J Phys Chem 1982;86:4470.

[213] Nakanishi T, Ohtani B, Uosaki K. J Phys Chem B 1998;102:1571.

[214] Robinson BH, Towey TF, Zourab S, Visser AJWG, Vanhoek A. Colloids Surf 1991;61:175.

[215] Tata M, Banerjee S, John VT, Waguespack Y, McPherson GL. Colloids Surf A Physicochem Eng Asp 1997;127:39.

[216] Qi LM, Ma JM, Cheng HM, Zhao ZG. Colloids Surf A Physicochem Eng Asp 1996;111:195.

[217] Ou DL, Seddon AB. Phys Chem Glasses 1998;39:154.

[218] Pang Q, Guo BC, Wang JN, Yang SH, Wang YQ, Ge WK, et al. Chem J Chin Univ 2004;25:1593.

[219] Pang Q, Guo BC, Yang CL, Yang SH, Gong ML, Ge WK, et al. J Cryst Growth 2004;269:213.

[220] Quinlan FT, Kuther J, Tremel W, Knoll W, Risbud S, Stroeve P. Langmuir 2000;16:4049.

[221] Hirai T, Watanabe T, Komasawa I. J Phys Chem B 2000;104:8962.

[222] Cao LX, Zhang JH, Ren SL, Huang SH. Appl Phys Lett 2002;80:4300.

[223] Hoener CF, Allan KA, Bard AJ, Campion A, Fox MA, Mallouk TE, et al. J Phys Chem 1992;96:3812.

[224] Gao XH, Cui YY, Levenson RM, Chung LWK, Nie SM. Nat Biotechnol 2004;22:969.

[225] Pellegrino T, Manna L, Kudera S, Liedl T, Koktysh D, Rogach AL, et al. Nano Lett 2004;4:703.

[226] Michalet X, Pinaud FF, Bentolila LA, Tsay JM, Doose S, Li JJ, et al. Science 2005;307:538.

[227] Medintz IL, Uyeda HT, Goldman ER, Mattoussi H. Nat Mater 2005;4:435.

[228] Gao XH, Yang LL, Petros JA, Marshal FF, Simons JW, Nie SM. Curr Opin Biotechnol 2005;16:63.

[229] Pinaud F, Michalet X, Bentolila LA, Tsay JM, Doose S, Li JJ, et al. Biomaterials 2006;27:1679.

[230] Winter JO, Liu TY, Korgel BA, Schmidt CE. Adv Mater 2001;13:1673.
[231] Jaiswal JK, Goldman ER, Mattoussi H, Simon SM. Nat Methods 2004;1:73.
[232] Larson DR, Zipfel WR, Williams RM, Clark SW, Bruchez MP, Wise FW, et al. Science 2003;300:1434.
[233] Akerman ME, Chan WCW, Laakkonen P, Bhatia SN, Ruoslahti E. Proc Natl Acad Sci U S A 2002;99:12617.
[234] Lim YT, Kim S, Nakayama A, Stott NE, Bawendi MG, Frangioni JV. Mol Imaging 2003;2:50.
[235] Larson DR, Zipfel W, Clark S, Bruchez M, Wise F, Webb WW. Biophys J 2003;84:23a.
[236] Henglein A. Chem Rev 1989;89:1861.
[237] Lin J, Zhou WL, O'Connor CJ. Mater Lett 2001;49:282.
[238] Chiang CL. J Colloid Interface Sci 2001;239:334.
[239] Chen FX, Xu GQ, Hor TSA. Mater Lett 2003;57:3282.
[240] Sohn BH, Choi JM, Yoo SI, Yun SH, Zin WC, Jung JC, et al. J Am Chem Soc 2003;125:6368.
[241] Zsigmondy R, Thiessen PA. Das kolloide gold, Akademische verlagsgesellschaft m.b.h., Leipzig, 1925.
[242] Reed JA, Cook A, Halaas DJ, Parazzoli P, Robinson A, Matula TJ, et al. Ultrason Sonochem 2003;10:285.
[243] Pol VG, Gedanken A, Calderon-Moreno J. Chem Mater 2003;15:1111.
[244] Okitsu K, Yue A, Tanabe S, Matsumoto H, Yobiko Y, Yoo Y. Bull Chem Soc Jpn 2002;75:2289.
[245] Okitsu K, Yue A, Tanabe S, Matsumoto H, Yobiko Y. Langmuir 2001;17:7717.
[246] Chen W, Cai WP, Zhang L, Wang GZ, Zhang LD. J Colloid Interface Sci 2001;238:291.
[247] Chen W, Cai WP, Liang CH, Zhang LD. Mater Res Bull 2001;36:335.
[248] Shimizu T, Teranishi T, Hasegawa S, Miyake M. J Phys Chem B 2003;107:2719.
[249] Teranishi T, Hasegawa S, Shimizu T, Miyake M. Adv Mater 2001;13:1699.
[250] Nakamoto M, Yamamoto M, Fukusumi M. Chem Commun 2002:1622.
[251] Liu SH, Han MY. Adv Funct Mater 2005;15:961.
[252] Huang HZ, Yang XR. Biomacromolecules 2004;5:2340.
[253] Schroedter A, Weller H. Angew Chem Int Ed Engl 2002;41:3218.
[254] Kneipp K, Kneipp H, Itzkan I, Dasari RR, Feld MS. J Phys Condens Matter 2002;14:R597.
[255] Bosnick KA, Jiang J, Brus LE. J Phys Chem B 2002;106:8096.
[256] Mann S, Shenton W, Li M, Connolly S, Fitzmaurice D. Adv Mater 2000;12:147.
[257] Mrksich M. Chem Soc Rev 2000;29:267.
[258] Bright RM, Walter DG, Musick MD, Jackson MA, Allison KJ, Natan MJ. Langmuir 1996;12:810.
[259] Hermanson GT. Bioconjugate techniques. San Diego: Academic Press; 1996.
[260] Paciotti GF, Myer L, Weinreich D, Goia D, Pavel N, McLaughlin RE, et al. Drug Deliv 2004;11:169.
[261] O'Neal DP, Hirsch LR, Halas NJ, Payne JD, West JL. Cancer Lett 2004;209:171.
[262] Waggoner A. Biochem Spectrosc 1995;246:362.
[263] Kuno M, Fromm DP, Hamann HF, Gallagher A, Nesbitt DJ. J Chem Phys 2000;112:3117.
[264] Derfus AM, Chan WCW, Bhatia SN. Nano Lett 2004;4:11.
[265] Hoshino A, Fujioka K, Oku T, Suga M, Sasaki YF, Ohta T, et al. Nano Lett 2004;4:2163.
[266] Yamazaki K, Tanaka A, Hirata M, Omura M, Makita Y, Inoue N, et al. J Occup Health 2000;42:169.